

doi: 10.12029/gc20200611002

李岩, 程春, 苏绍明, 高剑峰, 黄费新, 熊映志, 张岩, 黄华. 2023. 鄂东南地区金井咀金矿早白垩世闪长岩 Sr–Nd 及锆石 Hf 同位素研究[J]. 中国地质, 50(5): 1573–1585.

Li Yan, Cheng Chun, Su Shaoming, Gao Jianfeng, Huang Feixin, Xiong Yingzhi, Zhang Yan, Huang Hua. 2023. Sr–Nd and zircon Hf isotopic constraints on petrogenesis of the Early Cretaceous diorite in the Jinjingzui gold deposit, southeast Hubei Province[J]. Geology in China, 50(5): 1573–1585(in Chinese with English abstract).

## 鄂东南地区金井咀金矿早白垩世闪长岩 Sr–Nd 及 锆石 Hf 同位素研究

李岩<sup>1</sup>, 程春<sup>1</sup>, 苏绍明<sup>1,2</sup>, 高剑峰<sup>3</sup>, 黄费新<sup>1</sup>, 熊映志<sup>1,4</sup>, 张岩<sup>1</sup>, 黄华<sup>1</sup>

(1. 中国冶金地质总局矿产资源研究院, 北京 101300; 2. 中国冶金地质总局中南局, 湖北 武汉 430081; 3. 中国科学院地球化学研究所, 矿床地球化学国家重点实验室, 贵州 贵阳 550081; 4. 中国冶金地质总局中南地质勘查院, 湖北 武汉 430081)

**提要:**【研究目的】金井咀金矿床早白垩世闪长岩的岩石成因及岩浆起源对于讨论成岩成矿关系、完善区域成矿规律等问题具有重要意义。**【研究方法】**本文对矿区赋矿闪长岩开展了全岩 Sr–Nd 和锆石 Hf 同位素分析。**【研究结果】**金井咀闪长岩具有相对较高的  $^{87}\text{Sr}/^{86}\text{Sr}$  初始比值 (0.7059–0.7062), 负的  $\varepsilon_{\text{Nd}}(t)$  值 ( $-7.93 \sim -7.58$ ) 和锆石  $\varepsilon_{\text{Hf}}(t)$  值 ( $-12.2 \sim -6.5$ ), 表明岩浆形成于富集地幔的部分熔融, 后经历了演化分异, 在岩浆演化过程中可能存在一定程度的陆壳混染。**【结论】**通过与区域上已经发现的矿床对比发现, 金井咀矽卡岩型金矿床与鄂东南矿集区矽卡岩型金矿床具有相同的成岩成矿时代和类似的岩石成因及岩浆源区, 但是金井咀矿床金矿体主要赋存在闪长岩体内部, 这与其他矿床主要赋存在碳酸盐岩地层或岩体内外接触带明显不同。金井咀矿床的发现, 对于完善区域成矿规律, 指导金矿找矿勘查具有重要的意义。

**关 键 词:** Sr–Nd 同位素; 锆石 Hf 同位素; 闪长岩; 金井咀 Au 矿; 地质调查工程; 鄂东南

**创 新 点:**查明了金井咀金矿床早白垩世闪长岩的岩石成因和岩浆源区特征, 探讨了成岩成矿关系及, 为区域金矿找矿勘查提供新的思路。

中图分类号:P588.12; P597.1 文献标志码:A 文章编号:1000–3657(2023)05–1573–13

## Sr–Nd and zircon Hf isotopic constraints on petrogenesis of the Early Cretaceous diorite in the Jinjingzui gold deposit, southeast Hubei Province

LI Yan<sup>1</sup>, CHENG Chun<sup>1</sup>, SU Shaoming<sup>1,2</sup>, GAO Jianfeng<sup>3</sup>, HUANG Feixin<sup>1</sup>,  
XIONG Yingzhi<sup>1,4</sup>, ZHANG Yan<sup>1</sup>, HUANG Hua<sup>1</sup>

(1. Institute of Mineral Research, China Metallurgical Geology Bureau, Beijing 101300, China; 2. Centralsouth Bureau of China Metallurgical Geology Bureau, Wuhan 430081, Hubei China; 3. State Key Laboratory of Ore Deposit Geochemistry, Chinese Academy of Science, Guiyang 550081, Guizhou, China; 4. Institute of Centralsouth Geology Exploring, China Metallurgical Geology Bureau, Wuhan 430081, Hubei, China)

收稿日期:2020–06–11; 改回日期:2020–08–25

基金项目:国家重点研发计划(2016YFC0600207)和中国冶金地质总局矿产资源研究院自筹项目联合资助。

作者简介:李岩,男,1988年生,高级工程师,主要从事岩石学和矿床学研究;E-mail:liyan@cmgb.cn。

通讯作者:程春,男,1969年生,教授级高级工程师,主要从事矿床学研究;E-mail:chengchun@cmgb.cn。

**Abstract:** This paper is the result of geological survey engineering.

**[Objective]** The petrogenesis and magmatic origin of the early Cretaceous diorite in Jinjingzui gold deposit are of great significance for the diagenetic and metallogenic relations and perfecting the regional metallogenic regularity. **[Methods]** In this study we report the Sr–Nd and zircon Hf isotopic compositions of diorite in Jinjingzui deposit. **[Results]** The results show that the diorite has relative high initial  $^{87}\text{Sr}/^{86}\text{Sr}$  ratio (0.7059–0.7062), negative  $\varepsilon_{\text{Nd}}(t)$  values (−7.93–−7.58) and  $\varepsilon_{\text{Hf}}(t)$  values (−12.2–−6.5), suggesting the magma was derived from partial melting of an enrichment mantle, followed by magma differentiation. There may be continental crust contamination during magmatic evolution. **[Conclusions]** By comparison with reported deposit in cluster, Jinjingzui Au deposit is similar to these Au deposit at Edong cluster in rock- and ore-forming ages, petrogenesis and magma source. However, the gold orebody of Jinjingzui Au deposit mainly lay within the diorite body, which is obviously different from other deposits that lay internal or external contact zone of rocks. The discovery of Jinjingzui deposit is of great significance for perfecting regional metallogenic regularity and gold prospecting and exploration.

**Key words:** Sr–Nd isotopes; zircon Hf isotopes; diorite Jinjingzui Au deposit; geological survey engineering; southeast Hubei Province

**Highlights:** Identification of the petrogenesis and magmatic origin of the Early Cretaceous diorite in Jinjingzui gold deposit, and discussed the relationship between diagenesis and mineralization, providing a new idea for regional gold prospecting.

**About the first author:** LI Yan, male, born in 1988, senior engineer, mainly engaged in petrology and metallogeny survey; E-mail: liyan@cmgb.cn.

**About the corresponding author:** CHENG Chun, born in 1969, professor of engineering, mainly engaged in metallogeny survey; E-mail: chengchun@cmgb.cn.

**Fund support:** Supported by the National Key R&D Program of China (No.2016YFC0600207) and Science Foundation of Institute of Mineral Resources Research, China Metallurgical Geology Bureau.

## 1 引言

长江中下游地区资源储量巨大,是中国重要的斑岩–矽卡岩铜–铁–金–钨–钼成矿带(Mao et al., 2011; Pang et al., 2014; Zhou et al., 2015; Samake et al., 2018)。该带由鄂东南、九瑞、安庆—贵池、铜陵、宁芜、宁镇六大矿集区组成(图1),开发历史悠久,研究成果丰硕(Pan and Dong, 1999; Xie et al., 2011a; Mao et al., 2011)。鄂东南矿集区位于湖北省南部,隶属于长江中下游成矿带西段(图1)。已有的研究表明,鄂东南矿集区成矿元素以Fe、Cu、Au、Mo为主,且在空间上具有一定的分带性,北西部主要发育铁矿、铁铜矿,如程潮铁矿和金山店铁矿、铁山铁铜矿等;南东主要发育铜(金、钼)和W–Cu矿床,如铜绿山(Fe、Au)Cu矿床,鸡冠嘴铜金矿床、千家湾Cu、Au矿床、铜山口Cu–Mo矿和软家湾W–Cu矿等。

金井咀金矿位于鄂东南矿集区中部,金金属量5874 kg,矿体平均品位7.29 g/t,金理论地质储量达到大型规模,具有较大的成矿潜力(苏欣栋,1996;李新昊和谢桂青,2018)。然而,对于该矿床成矿岩

体及矿床成因的研究仍然比较少。苏欣栋(1996)对该矿床地质特征的研究认为,成矿作用与矿区闪长岩有关,成矿类型为蚀变闪长岩筒型金矿床,成岩、成矿物质可能同源,但缺少同位素证据支持。陈文等(2012)认为该矿床具有典型矽卡岩型矿床特征,金矿化与矽卡岩化关系密切,为矽卡岩型金矿床。本文对与金井咀金矿床成矿关系密切的闪长岩开展了全岩Sr–Nd及锆石Hf同位素研究,揭示岩浆源区特征,查明岩石成因,并结合区域成矿特征,探讨了成岩成矿关系及对区域成矿的意义。

## 2 区域地质背景

鄂东南矿集区位于长江中下游成矿带的西端(图2),隶属于长江中下游成矿带中亚带(周涛发等,2017)。金井咀矿床位于湖北省大冶市,距离大冶市区南东约2 km。区域大地构造位置属扬子克拉通北缘,毗邻大别造山带(纪敏等,2018),处于北西向襄阳—广济断裂、北东向商麻—团风—梁子湖断裂及北东向郯庐断裂夹持地带(周涛发等,2017)。区域广泛出露寒武系到第四系,缺失中、下泥盆统和上侏罗统,其中三叠系碳酸盐岩为区内矽

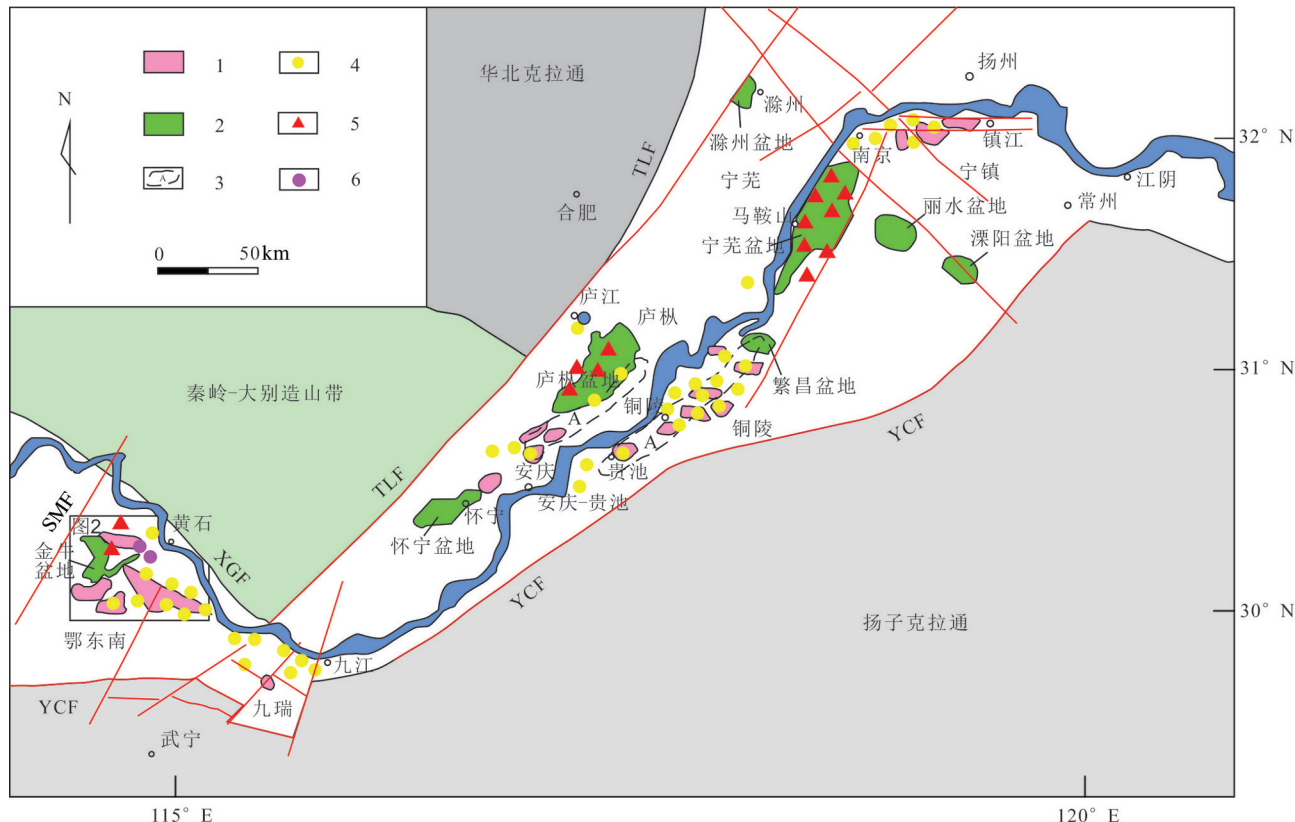


图1 长江中下游成矿带地质矿产简图(据常印佛等,1991; Xie et al., 2011b)

1—晚侏罗—早白垩世花岗岩(156~137 Ma);2—白垩纪火山岩和次火山岩(<135 Ma);3—A型花岗岩带(127~125 Ma);4—斑岩—矽卡岩—层控Cu-Au-Mo矿床(>135 Ma);5—Fe矿床;6—矽卡岩型Fe-Cu矿床(>135 Ma);TLF—郯庐断裂;XGF—襄樊—广济断裂;YCF—阳新—常州断裂;SMF—商麻—团风—梁子湖断裂

Fig.1 Sketch map of Middle-Lower reaches of the Yangtze River metallogenic belt (after Chang Yinfo et al., 1991; Xie et al., 2011b)

1—Late Jurassic-Early Cretaceous granitoids (156~137 Ma); 2—Cretaceous volcanic and subvolcanic rocks(<135 Ma); 3—A-type granitoids belt; 4—Porphyry-skarn-stratabound Cu-Au-Mo deposits (>135 Ma); 5—Fe deposits; 6—Skarn Fe-Cu deposits (>135 Ma); TLF—Tancheng-Lujiang fault; XGF—Xiangfan-Guangji fault; YCF—Yangxiong-Changzhou fault; SMF—Shangma-Tuanfeng-Liangzihu fault

卡岩型矿床的主要围岩(李新昊等,2018)。区域发育印支期区域性NW—NNW向断裂,控制区域成岩作用,燕山期以发育较小规模的NE—NNE向断裂为特征(舒全安等,1992)。区内出露包括鄂城、铁山、金山店、灵山、殷祖、阳新6个不同大小的岩体,岩性主要为闪长岩和石英闪长岩类(图2),此外还发育众多小岩体(丰山花岗闪长斑岩、铜山口花岗闪长岩等)。这些岩体成岩时代为晚侏罗世—早白垩世(Xie et al., 2011a, b; 陈富文等, 2012; 姚磊等, 2013)。

### 3 矿床地质特征

金井咀矿区位于阳新岩体西北缘北侧,大冶复式向斜南翼(陈文等,2012)。矿区第四系沉积物

覆盖严重(超过80%),钻孔工程揭露,在中部可见到下三叠统大冶群第二—第五段地层,南部可见到大冶群第五—第七段地层,主要为薄层—厚层状大理岩、白云岩、白云质大理岩。矿区发育的岩体主要为闪长岩,其次为闪长斑岩,闪长斑岩多分布于小岩体的边部,与闪长岩呈相变关系。矿区主要构造线为北东向、北西向,其中金井咀闪长岩体及金矿床受北东向倒转背斜与北西向断裂构造控制,产于构造交汇部位(图3a)。

金井咀金矿床由8个大小不一的金矿体组成,其中以①号金矿体规模最大,分布在第9~14号勘探线之间,产出标高为7~374 m,控制的储量近8 t。除⑧号矿体赋存在岩体顶部接触带,其余矿体主要呈不规则不完整的环筒形围绕在似筒状小岩体内

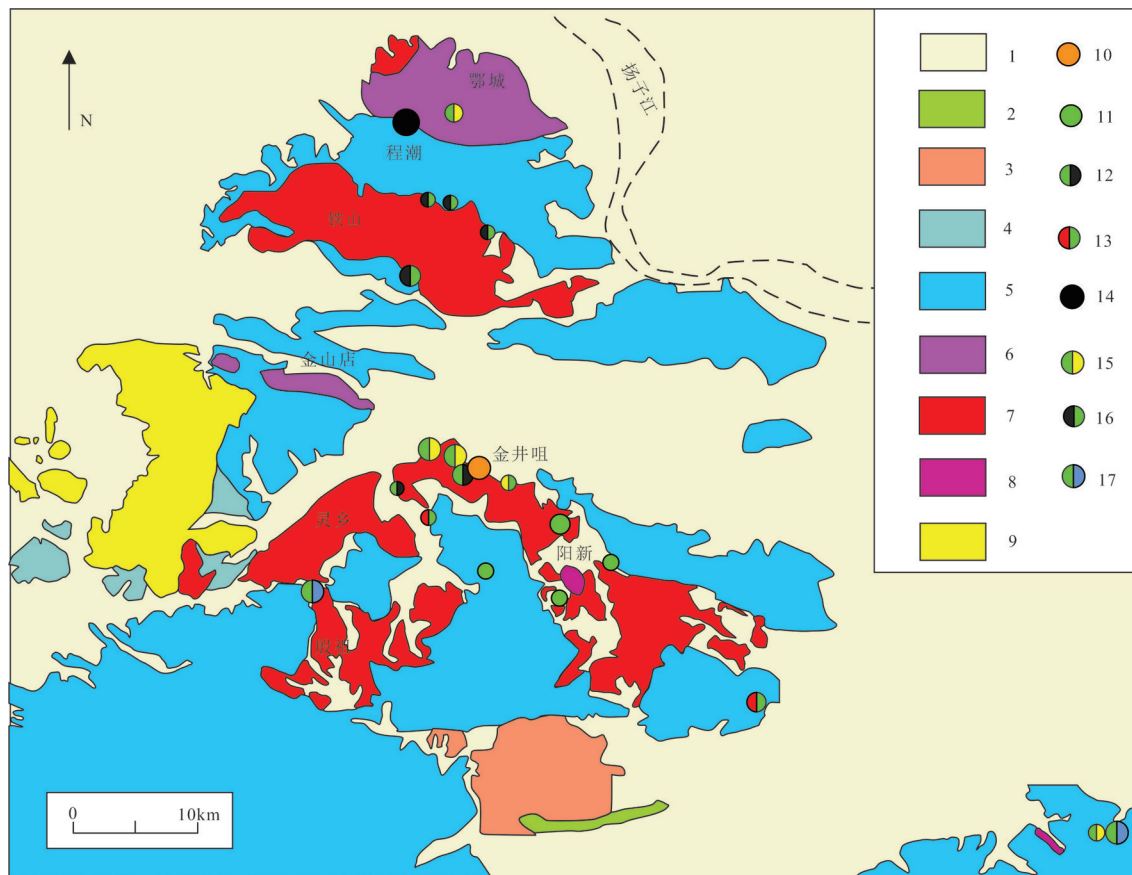


图2 鄂东南矿集区主要岩体及矿床分布分图(据李新昊等,2018修改)

1—第四系;2—古近纪玄武岩;3—晚白垩世—新近纪红层;4—晚三叠世—中侏罗世碎屑岩;5—寒武纪—中三叠世碎屑岩和碳酸盐岩;6—白垩纪中期火山岩;7—白垩纪中期花岗岩—石英二长岩—闪长岩;8—早白垩世早期辉长岩—石英闪长岩—闪长岩;9—早白垩世早期花岗闪长斑岩和花岗斑岩;10—Au矿床;11—Cu矿床;12—Cu-Fe矿床;13—W-Cu矿床;14—Fe矿床;15—Cu-Au矿床;16—Fe-Cu矿床;17—Cu-Mo矿床

Fig.2 Distribution map of main igneous rocks and deposits in southeast Hubei Province(modified from Li Xinhao et al., 2018)  
 1—Quaternary; 2—Paleogene basalt; 3—Late Cretaceous – Neogene red layer; 4—Late Triassic – Middle Jurassic clastic rocks; 5—Cambrian – Middle Triassic clastic rocks and carbonate rocks; 6—Mid-Cretaceous volcanic rocks; 7—Middle Cretaceous granite–quartz monozodiorite– diorite; 8—Early cretaceous gabbro – quartz diorite – diorite; 9—Granodiorite porphyry and granoporphry in early cretaceous; 10—Au deposit; 11—Cu deposit; 12—Cu–Fe deposit; 13—W–Cu deposit; 14—Fe deposit; 15—Cu–Au deposit; 16—Fe–Cu deposit; 17—Cu–Mo deposit

侧、或呈脉状分布于小岩体中部(图3b)。

金井咀矿床矿石主要以浸染状构造和脉状构造为主(图4a,b),局部可见致密块状构造和角砾状构造。矿石结构主要包括半自形—自形粒状结构、他形粒状结构、胶状结构、交代熔蚀结构、固溶体分离结构、变胶结构、碎裂结构等。已确定的矿物超过30种,其中金属矿物有14种,按成分可分为氧化物、硫化物、自然元素及碲化物等。金属氧化物主要为磁铁矿和赤(褐)铁矿;硫化物主要为黄铁矿、胶黄铁矿、白铁矿、磁黄铁矿、黄铜矿、斑铜矿、蓝辉铜矿、铜蓝、方铅矿和闪锌矿等;自然元素主要为

金、银互化系列矿物;碲化物主要为碲铅矿。脉石矿物有中长石、钾长石、石英、角闪石、黑云母、石榴子石、透辉石、柱石、方解石、蒙脱石、水云母、绢云母等(图4c,d)。金的赋存状态包括显微金、次显微金和分散金三种,以自然金为主,少量为金银矿。显微金形态主要有浑圆状、板片状、叶片状、树枝状、棱角状、多角状和不规则状。依据金与其他矿物关系可将显微金的产出特征分为粒间—裂隙金及包裹金两种。前者为产于矿物颗粒间隙中的粒间金和矿物内部裂隙中的裂隙金,颗粒较粗,很容易解离出来。后者粒径细小,不易解离,主要包裹

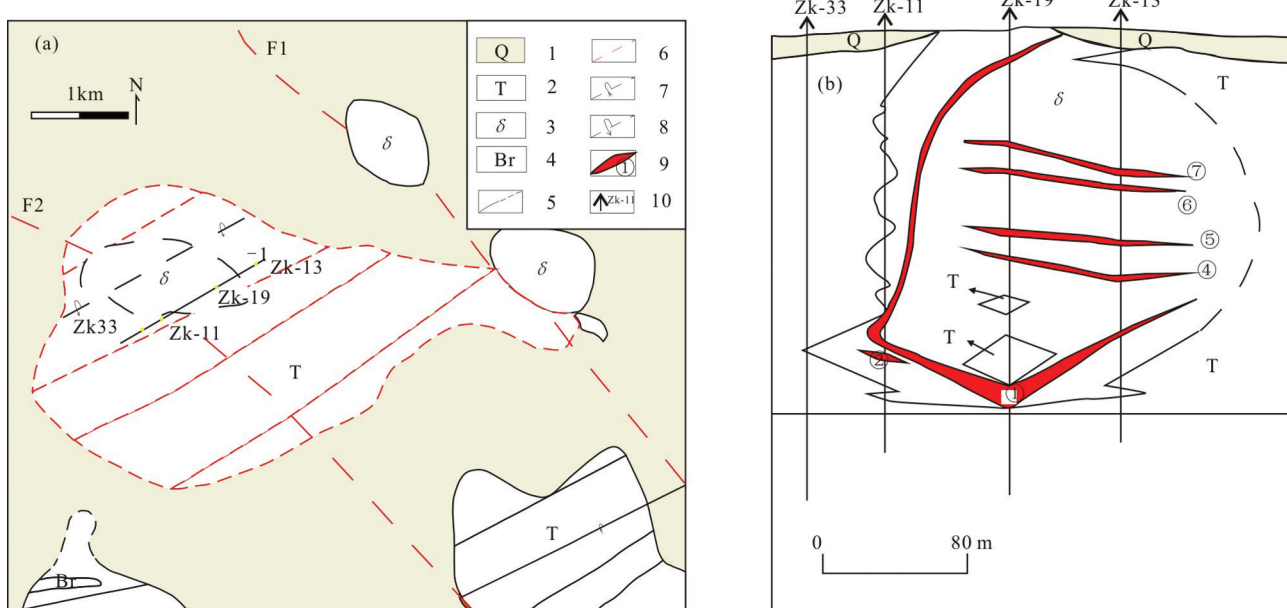


图3 金井咀矿区地质图(a)及矿体剖面图(b)

1—第四系;2—下三叠统大冶群;3—闪长岩;4—构造角砾岩;5—实测及推断地质界线;6—实测及推断断层;7—倒转向斜;8—倒转背斜;  
9—矿体及编号;10—钻孔及编号

Fig.3 Geological map of Jingjingzui deposit(a) and ore body's section(b) showing the distribution of the orebody  
1—Quaternary; 2—Lower Triassic Daye Group; 3—Diorite; 4—Tectonic breccia; 5—Measured and inferred geological boundaries;  
6—Measured and inferred faults; 7—Overturned syncline; 8—Overturned anticline; 9—Orebodyand number; 10—Drill and number

在黄(白)铁矿和碲铅矿等矿物中。与金矿化有关的围岩蚀变主要包括矽卡岩化和硅化。根据野外观察矿脉间的穿切关系、矿物组合和相邻矿物的结

构/生长关系,金井咀金矿床大致经历了四个不同成岩成矿期,包括矽卡岩期,石英硫化物期,碳酸盐期和表生氧化期,各期主要矿物生成顺序见图5。岩

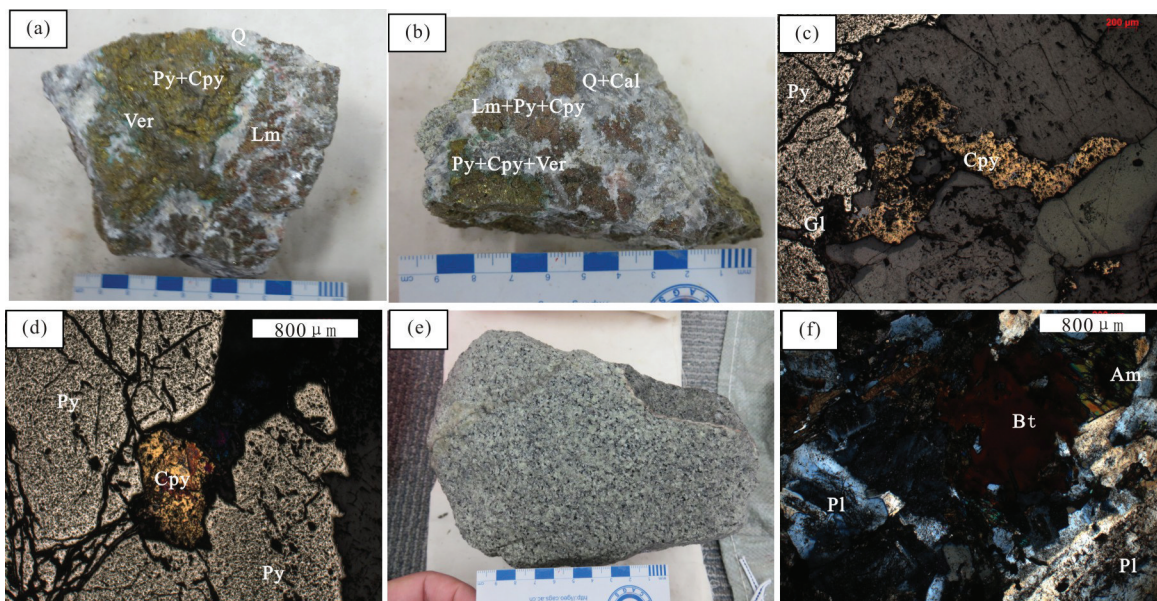


图4 金井咀矿床矿石及闪长岩手标本及镜下照片

Q—石英;Py—黄铁矿;Cpy—黄铜矿;Gl—方解石;Ver—铜绿;Cal—方解石;Lm—褐铁矿;Pl—斜长石;Am—角闪石;Bt—黑云母

Fig.4 Photos of ore and diorite in Jingjingzui deposit

Q—Quartz; Py—Pyrite; Cpy—Chalcopyrite; Gl—Galena; Ver—Verdigris; Cal—Calcite; Lm—Limonite; Pl—Plagioclase; Am—Amphibole; Bt—Biotite

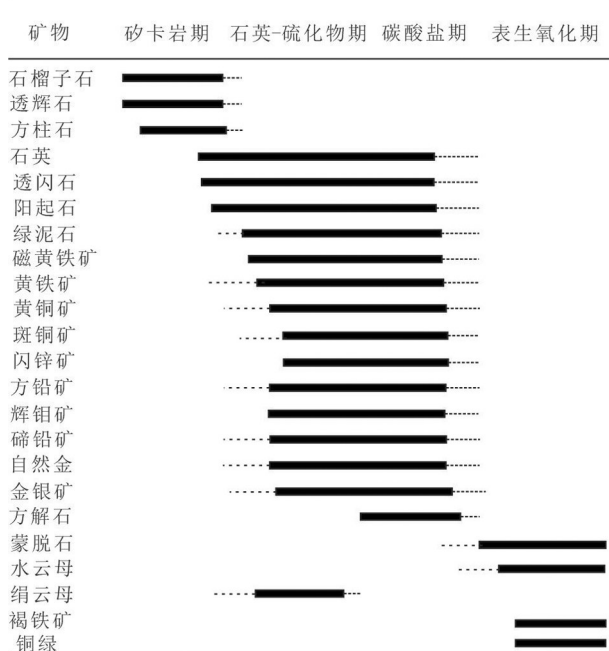


图5 金井咀矿床矿物生成序列图

Fig.5 Paragenetic sequence of minerals from the Jinjingzui Au deposit

浆侵入成岩期主要形成闪长(斑)岩岩筒,在其结晶成岩过程中,与围岩大理岩接触交代形成矽卡岩,待两者形成后,又发生岩浆期后的热液蚀变(矽卡岩化、含金硫化物及碳酸盐化、黏土化等),并伴随金矿化,形成含金蚀变闪长(斑)岩型金矿石,随后又发生表生氧化作用,长石变为蒙脱石、高岭土、水云母、铁铜硫化物,金属氧化物变成赤(褐)铁矿,形成了赤(褐)铁矿化含金蚀变闪长(斑)岩型金矿石。

#### 4 样品及分析方法

锆石和岩石粉末来自于3件新鲜的闪长岩样品(JJZ-7、JJZ-8和JJZ-9),样品均采自金井咀矽卡岩矿床-280 m平硐。闪长岩为灰色—灰绿色,半自形粒状结构,块状构造。主要成分为斜长石(60%~80%)、角闪石(3%~8%)、辉石(2%~7%),次为黑云母(3%~5%)、石英(1%~3%)(图4e,f);副矿物有榍石、锆石和磷灰石。

锆石制靶及阴极发光照相在北京锆年领航科技有限公司完成,锆石U-Pb定年在北京燕都中实测试技术有限公司完成。本次锆石U-Pb同位素定年利用LA-ICP-MS分析完成。束斑选择25 μm,粗体采用标准锆石GJ-1作外标进行同位素分馏校

正,视测试情况每分析5~10个样品点,分析2次GJ-1。激光剥削系统为New Wave UP213, ICP-MS为布鲁克M90。采用He气作为剥蚀过程中的载体,氩作为补偿气以调节灵敏度,二者在进入ICP之前在Y型接口处混合。每个时间分辨分析数据空白信号20~30 s,样品信号为50 s。

Sr-Nd和锆石Hf同位素在北京燕都中实测试技术有限公司完成。Sr和Nd同位素使用Thermo Fisher Scientific多接收电感耦合等离子体质谱仪Neptune Plus MC-ICP-MS分别测定<sup>87</sup>Sr/<sup>86</sup>Sr值和<sup>143</sup>Nd/<sup>144</sup>Nd值,根据<sup>88</sup>Sr/<sup>86</sup>Sr值(8.373209)和<sup>143</sup>Nd/<sup>144</sup>Nd值(0.7218)按照指数规律对测定的<sup>87</sup>Sr/<sup>86</sup>Sr值和<sup>143</sup>Nd/<sup>144</sup>Nd值进行在线质量分馏校正。<sup>87</sup>Sr/<sup>86</sup>Sr值和<sup>143</sup>Nd/<sup>144</sup>Nd值的不确定度为2σ,仅包含质谱测定的不确定度。本次用于分析Sr、Nd同位素分析的样品同时开展了主量和微量元素分析。锆石原位Lu-Hf同位素由美国Thermofisher公司生产的Neptune-plus MC-ICP-MS与NewWave UP213激光烧蚀进样系统完成测试的。测试过程中使用He作为剥蚀剥蚀物质载气,采用频率为8 Hz,能量密度为16 J/cm<sup>2</sup>的激光强剥蚀31 s,剥蚀束斑为30 μm。测试时,由于锆石中的<sup>176</sup>Lu/<sup>177</sup>Hf比值极其低(一般小于0.002),<sup>176</sup>Lu对<sup>176</sup>Hf的同位素干扰可以忽略不计。每个测试点的<sup>173</sup>Yb/<sup>172</sup>Yb平均值用于计算Yb的分馏系数,然后再扣除<sup>176</sup>Yb对<sup>176</sup>Hf的同质异位素干扰。<sup>173</sup>Yb/<sup>172</sup>Yb的同位素比值为1.35274。获得标准锆石Plesovice的<sup>176</sup>Hf/<sup>177</sup>Hf值为0.282430~0.282526,与推荐值(0.282484±17)在误差范围内一致(Elhlou et al., 2006)。

#### 5 分析结果

##### 5.1 锆石U-Pb同位素

金井咀闪长岩锆石结晶较好,呈长柱状晶型,长宽比为1:1~1:3。锆石阴极发光照片可见清晰的岩浆锆石震荡环带(图6),不具有明显的核-幔结构,亦无后期变质壳,表明其为典型的岩浆锆石。对两个样品分别选取25颗锆石进行U-Pb同位素测试,测试结果见表1。锆石Th和U含量总体变化不大,Th/U比为1.0~3.5。样品JJZ-7获得的25个数据,其中24个测点谐和度达到95%,其<sup>206</sup>Pb/<sup>238</sup>U年龄为(141.1±0.4) Ma,加权平均年龄为(141.1±0.9)

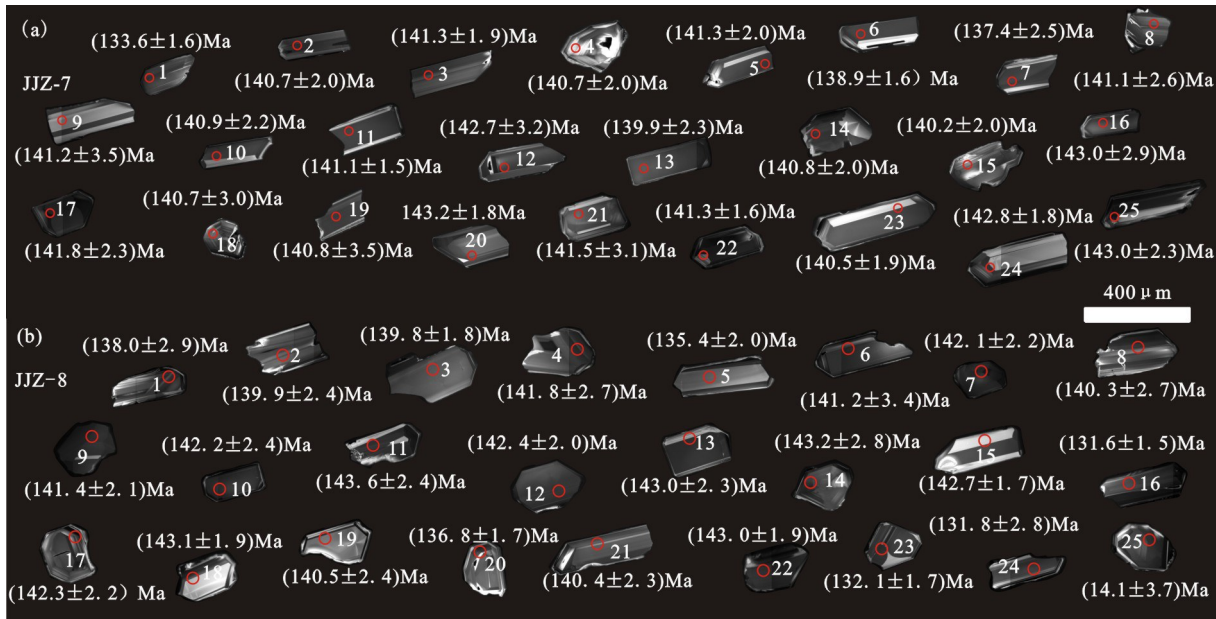


图6 金井咀闪长岩锆石阴极发光照片及测年结果

Fig.6 Cathodoluminescence (CL) images of zircons from Jinjingzui diorite and analytical spots ages

Ma(图7a);样品JJZ-8获得的25个数据,其中20个测点谐和度达到95%,其 $^{206}\text{Pb}/^{238}\text{U}$ 年龄为(141.8±0.5) Ma,加权平均年龄为(141.7±1.0) Ma(图7b)。

## 5.2 Sr-Nd同位素

本文对金井咀闪长岩的3件代表性样品进行了Rb-Sr、Sm-Nd同位素分析,分析结果见表2。 $^{87}\text{Sr}/^{86}\text{Sr}$ 值分布在0.705937~0.706219,  $\varepsilon_{\text{Nd}}(t)$ 值为-7.93~-7.58,平均值为-7.78。对应的 $T_{\text{DM}}$ 值为1410~1445 Ma。

## 5.3 锆石Lu-Hf同位素

选取已经开展了U-Pb同位素分析锆石的不同部位进行锆石Lu-Hf同位素分析,分析结果见表3,Hf同位素总体成分相对均一,样品JJZ-7锆石( $^{176}\text{Hf}/^{177}\text{Hf}$ )值介于0.282351~0.282513,平均值为0.282425,  $\varepsilon_{\text{Hf}}(t)$ 值变化范围为-12.2~-6.5,平均值为-9.61,一阶段模式年龄 $t_{\text{DM}}$ 为1136~1394 Ma,二阶段模式年龄 $t_{\text{DMC}}$ 为1580~1944 Ma。样品JJZ-8锆石( $^{176}\text{Hf}/^{177}\text{Hf}$ )值介于0.282364~0.282451,平均值为0.282416,  $\varepsilon_{\text{Hf}}(t)$ 值变化范围为-11.7~-8.7,平均值为-9.9,一阶段模式年龄 $t_{\text{DM}}$ 为1189~1361 Ma,二阶段模式年龄 $t_{\text{DMC}}$ 为1720~1914 Ma。

## 5.4 岩石成因

具有相对较高的 $^{87}\text{Sr}/^{86}\text{Sr}$ 初始比值(0.705937~

0.706219),负的 $\varepsilon_{\text{Nd}}(t)$ 值(-7.93~-7.58),与区域上同时代铜、金矿化有关的中酸性侵入岩相似,在 $\varepsilon_{\text{Nd}}(t)$ - $(^{87}\text{Sr}/^{86}\text{Sr})$ 图解中落入富集地幔范围(图8)(Li et al., 2008; Xie et al., 2011b; 丁丽雪等,2018)。金井咀闪长岩的锆石 $^{176}\text{Hf}/^{177}\text{Hf}$ 值介于0.282360~0.282526,主要分布于下地壳与球粒陨石演化线之间(图9a); $\varepsilon_{\text{Hf}}(t)$ 值介于-12.2~-6.5,明显不同于大洋玄武岩( $\varepsilon_{\text{Hf}}(t)>0$ )(Hamelin et al., 2010),因此排除了大洋板片部分熔融的可能性,主要分布在亏损地幔和地壳演化线之间(图9b); $f_{\text{Lu/Hf}}$ 值介于-0.94~0.86,明显低于铁镁质地壳( $f_{\text{Lu/Hf}}=0.34$ )和硅铝质地壳( $f_{\text{Lu/Hf}}=0.72$ )(Vervoort et al., 1996; Amelin et al., 1999),暗示在岩浆演化过程中可能存在一定的陆壳混染(丁丽雪等,2018; 龚雪静等,2019)。而在锆石的CL图像中,并未发现古老的继承锆石,说明陆壳混染并不重要。

前人研究表明,鄂东南地区早白垩世岩浆岩成因主要包括三种成因:(1)靠近洋中脊的热的俯冲板片或蚀变洋壳的部分熔融(Ling et al., 2009);(2)拆沉或增厚下地壳的部分熔融(Wang et al., 2004);(3)由年轻的地幔和较老的地壳物质混合而成或富集地幔部分熔融,并经历了不同程度的地壳同化混染和分离结晶而成(Li et al., 2008; Xie et al., 2011a)。前两种成因的岩石一般具有埃达克质岩石



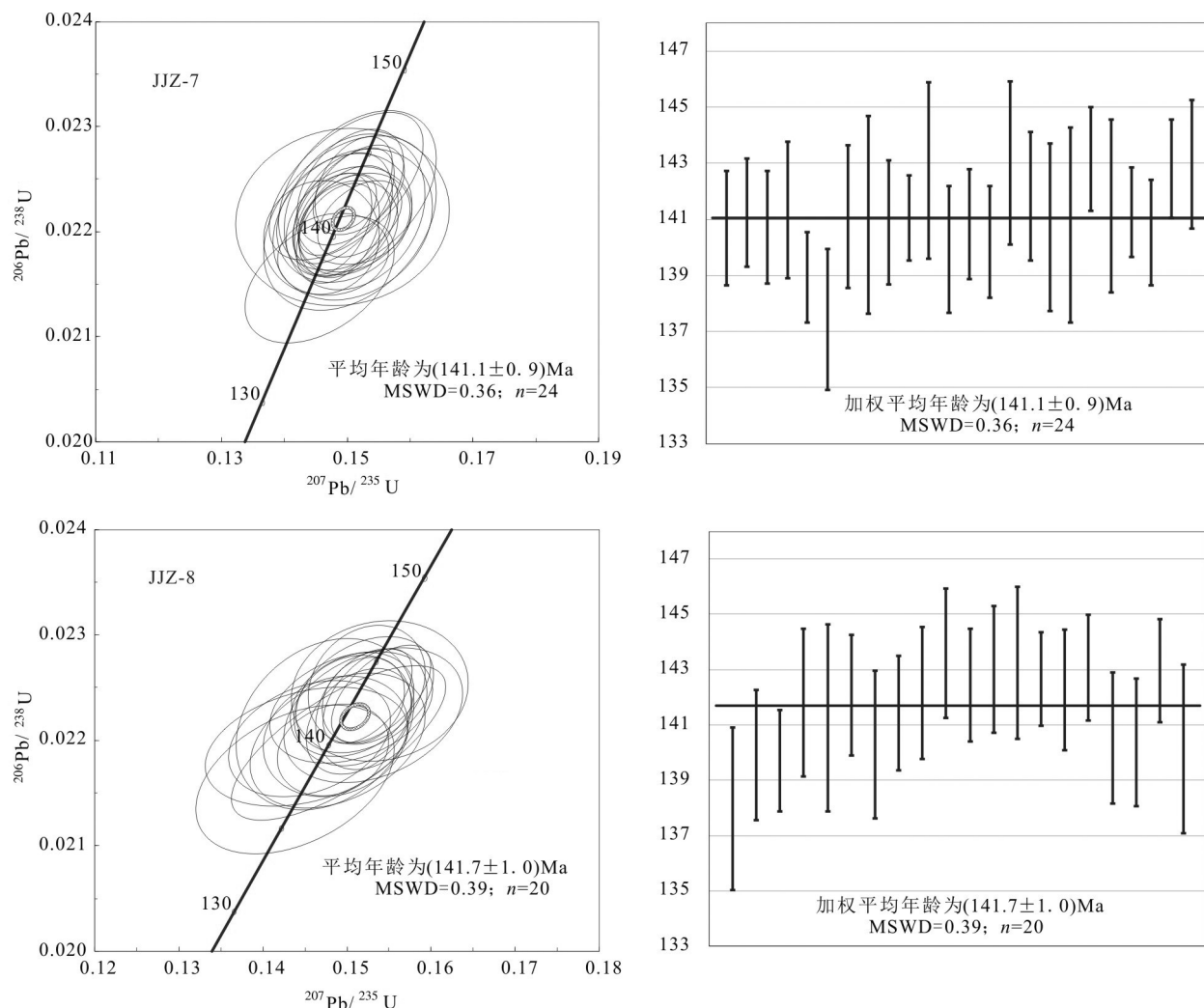


图7 金井咀金矿闪长岩锆石U-Pb年龄谐和图  
 Fig.7 Concordia diagram of zircon U-Pb age of the diorite in the Jinjingzui Au deposit

特征。金井咀闪长岩与鄂东南地区早白垩世与铜金成矿有关的闪长岩类岩石具有类似的同位素组成,如铜绿山铜铁金矿床石英闪长岩( $\varepsilon_{\text{Hf}}(t) = -8.9 \pm 1.1$ ,  $\varepsilon_{\text{Nd}}(t) = -3.8$ )和鸡冠嘴铜金矿床石英闪长岩( $\varepsilon_{\text{Hf}}(t) = -8.9 \pm 0.6$ ,  $\varepsilon_{\text{Nd}}(t) = -6.7$ ),这些岩石不具有埃达克岩的特征,起源于富集地幔的部分熔融(Xie et al., 2011a)。加之,金井咀闪长岩Mg<sup>#</sup>值(30.18~39.17)明显低于地幔橄榄岩平衡溶体的Mg<sup>#</sup>值(70~80)(Falloon et al., 1997),其成分不能代表原始与橄榄岩矿物组合平衡的熔体,因此,不可能是地幔橄榄岩经低温部分熔融直接形成,应是经富集地幔源区部分熔融形成玄武质岩浆,后经历了岩浆演化分异。

### 5.5 成岩、成矿关系

本文用于测试的5辉钼矿样品产于矽卡岩中,

形成于石英硫化物阶段,与金近同期形成。辉钼矿颗粒较细,且形成时代较年轻,未受到失耦作用影响(杜安道等, 2007),获得5件样品模式年龄加权平均值为( $139.0 \pm 1.1$ ) Ma,等时线年龄为( $138.5 \pm 2.7$ ) Ma。金井咀闪长岩锆石U-Pb测年结果显示其形成于141~142 Ma,成岩成矿时代趋于一致。此外,金井咀金矿床的金矿体空间上与闪长岩体紧密共生,主要呈不规则不完整的环筒形围绕在似筒状小岩体内侧、或呈脉状分布于小岩体中部。此外,金井咀矿床黄铁矿黄铁矿 $\delta^{34}\text{S}$ 值集中于-2.4‰~8.4‰,及较高的Re含量( $847.91 \times 10^{-6}$ ~ $2018.58 \times 10^{-6}$ ),暗示成矿物质主要来源于岩浆,且有较多的地幔物质参与成矿。以上证据表明金井咀矽卡岩型金矿床在空间与时间上与矿区闪长岩关系密切,

**表2 金井咀闪长岩 Sr–Nd 同位素组成**  
**Table 2 Sr–Nd isotopic compositions of Jingjingzui diorite**

样品号	JJZ-7	JJZ-8	JJZ-9
Sm/ $^{106}$ Sm	9.79	10.34	9.59
Nd/ $^{106}$ Nd	58.78	60.81	55.13
$^{143}\text{Sm}/^{144}\text{Nd}$	0.100612	0.102738	0.105125
$^{143}\text{Nd}/^{144}\text{Nd}$	0.512249	0.512237	0.512231
$2\sigma$	0.000009	0.000007	0.000008
Rb/ $^{106}$ Rb	60.74	71.62	105.5
Sr/ $^{106}$ Sr	1815	1961	1661
$^{87}\text{Rb}/^{86}\text{Sr}$	0.096836	0.10568	0.183789
$^{87}\text{Sr}/^{86}\text{Sr}$	0.70641	0.70615	0.706588
$2\sigma$	0.000007	0.000007	0.000007
T/Ma	141	142	141
$(^{87}\text{Sr}/^{86}\text{Sr})_i$	0.706216	0.705937	0.706219
$(^{143}\text{Nd}/^{144}\text{Nd})_i$	0.512157	0.512142	0.512134
$\varepsilon_{\text{Nd}}(t)$	-7.58	-7.82	-7.93
$T_{\text{DM}}/\text{Ma}$	1215	1256	1291
$T_{\text{EDM}}/\text{Ma}$	1410	1433	1445

注:测试单位:北京燕都中实测试技术有限公司;测试方法:MC–ICP–MS;实验仪器:Neptune Plus。

矿区闪长岩可能为该矿床的主要物源。

## 5.6 地质意义

谢桂青等(2006, 2008)认为,长江中下游地区存在两期重要的成矿事件,成矿时代集中于132~145 Ma和123~125 Ma,鄂东南矿集区成矿作用主要发生于第一期成矿事件。大量的高精度同位素年代学数据显示,研究区内成岩成矿作用具有一定的对应关系,两者为同时相伴发生。Xie et al.

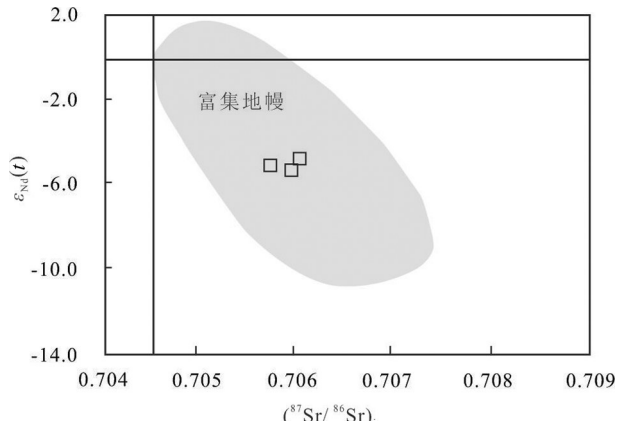


图8 金井咀闪长岩( $^{87}\text{Sr}/^{86}\text{Sr}$ ) $_i$ – $\varepsilon_{\text{Nd}}(t)$ 图(据Xie et al., 2011a)

Fig.8 ( $^{87}\text{Sr}/^{86}\text{Sr}$ ) $_i$ – $\varepsilon_{\text{Nd}}(t)$  diagram of diorite in Jingjingzui(after Xie et al., 2011a)

(2011a)研究发现鄂东南矿集区在136~143 Ma发育大量辉长岩、闪长岩及石英闪长岩,并伴生137~144 Ma的矽卡岩型Cu–Fe、Fe–Cu以及Au–Cu矿床。

如铜绿山(铁金)铜矿床形成于137.3~140.3 Ma(Xie et al., 2011b),矿区及周围中酸性岩浆岩形成时代为138.4~144.2 Ma(Li et al., 2010; Yang et al., 2014; 张世涛等, 2018);鸡冠嘴(铜)金矿床形成于138.2 Ma(谢桂青等, 2009),矿区石英闪长岩形成于139 Ma(Xie et al., 2011a),桃花嘴金(铜)矿床形于139.4~139.9 Ma,矿区石英闪长玢岩形成于139.3 Ma。金井咀矽卡岩型金矿床与上述矽卡岩型金矿床具有相同的成岩成矿时代,全岩Sr–Nd同位素及锆石Hf同位素具有类似的特征(Xie et al., 2011a),

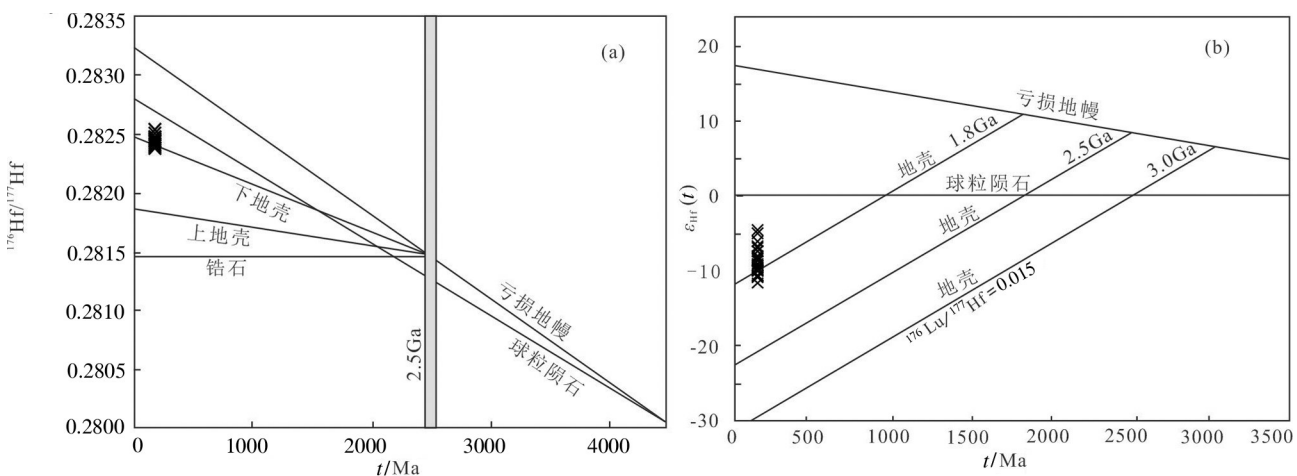


图9 锆石Hf同位素特征图(底图引自Vervoort et al., 1996)  
Fig.9 Hf isotopic composition of zircon (after Vervoort et al., 1996)

表3 金井咀闪长岩锆石Hf同位素组成

Table 3 Zircon Hfisotopic composition of diorite in Jinjingzui

测点号	年龄/Ma	$^{176}\text{Yb}/^{177}\text{Hf}$	$^{176}\text{Lu}/^{177}\text{Hf}$	$^{176}\text{Hf}/^{177}\text{Hf}$	$2\sigma$	$(^{176}\text{Hf}/^{177}\text{Hf})_i$	$\varepsilon_{\text{Hf}}(0)$	$\varepsilon_{\text{Hf}}(t)$	$t_{\text{DM}}/\text{Ma}$	$t_{\text{DMC}}/\text{Ma}$	$f_{\text{Lu/Hf}}$
JJZ-7-01	141	0.179750	0.004762	0.282526	0.000026	0.282513765	-9.1	-6.46	1140	1580	-0.86
JJZ-7-02	141	0.133944	0.003545	0.282382	0.000021	0.282372744	-14.2	-11.45	1317	1895	-0.89
JJZ-7-03	141	0.079841	0.002226	0.282445	0.000020	0.282439369	-12.0	-9.09	1179	1746	-0.93
JJZ-7-04	141	0.114238	0.003089	0.282381	0.000021	0.282372693	-14.3	-11.45	1302	1895	-0.91
JJZ-7-05	141	0.140991	0.003854	0.282429	0.000023	0.282418687	-12.6	-9.82	1258	1793	-0.88
JJZ-7-06	141	0.144343	0.003880	0.282393	0.000022	0.282382592	-13.9	-11.10	1314	1873	-0.88
JJZ-7-07	141	0.089769	0.002465	0.282418	0.000021	0.282411042	-13.0	-10.10	1227	1810	-0.93
JJZ-7-08	141	0.071973	0.001986	0.282360	0.000019	0.28235438	-15.0	-12.10	1294	1936	-0.94
JJZ-7-09	141	0.130178	0.003564	0.282485	0.000020	0.282475365	-10.6	-7.82	1164	1666	-0.89
JJZ-7-10	141	0.153904	0.004105	0.282515	0.000021	0.282503935	-9.6	-6.81	1136	1602	-0.88
JJZ-7-11	141	0.126784	0.003453	0.282452	0.000021	0.282443259	-11.8	-8.96	1209	1738	-0.90
JJZ-7-12	141	0.131524	0.003598	0.282436	0.000022	0.282426434	-12.3	-9.55	1238	1775	-0.89
JJZ-7-13	141	0.140454	0.003800	0.282460	0.000020	0.282449684	-11.5	-8.73	1210	1723	-0.89
JJZ-7-14	141	0.182363	0.004811	0.282364	0.000027	0.282351086	-14.9	-12.22	1395	1944	-0.86
JJZ-7-15	141	0.097339	0.002647	0.282463	0.000021	0.282456061	-11.4	-8.50	1166	1709	-0.92
JJZ-8-01	142	0.070626	0.002029	0.282422	0.000019	0.282416314	-12.8	-9.89	1206	1797	-0.94
JJZ-8-02	142	0.163773	0.004429	0.282376	0.000026	0.282364152	-14.5	-11.73	1361	1914	-0.87
JJZ-8-03	142	0.136201	0.003736	0.282419	0.000023	0.282409544	-12.9	-10.13	1268	1812	-0.89
JJZ-8-04	142	0.141812	0.003843	0.282461	0.000025	0.282450742	-11.5	-8.67	1209	1720	-0.88
JJZ-8-05	142	0.100944	0.002767	0.282402	0.000024	0.28239443	-13.6	-10.66	1260	1846	-0.92
JJZ-8-06	142	0.115204	0.003084	0.282457	0.000023	0.282449247	-11.6	-8.72	1189	1723	-0.91
JJZ-8-07	142	0.135582	0.003651	0.282421	0.000021	0.282411526	-12.9	-10.06	1262	1808	-0.89
JJZ-8-08	142	0.114259	0.003138	0.282444	0.000023	0.282435868	-12.1	-9.19	1210	1753	-0.91
JJZ-8-09	142	0.145644	0.003979	0.282449	0.000022	0.282438106	-11.9	-9.12	1233	1749	-0.88
JJZ-8-10	142	0.150205	0.004229	0.282434	0.000021	0.282422311	-12.4	-9.67	1265	1784	-0.87
JJZ-8-11	142	0.123209	0.003313	0.282422	0.000021	0.282413684	-12.8	-9.98	1249	1803	-0.90
JJZ-8-12	142	0.118924	0.003210	0.282441	0.000021	0.28243257	-12.2	-9.31	1217	1761	-0.90
JJZ-8-13	142	0.130546	0.003453	0.282396	0.000022	0.282386497	-13.8	-10.94	1294	1864	-0.90
JJZ-8-14	142	0.139072	0.003762	0.282405	0.000022	0.282395441	-13.4	-10.62	1290	1844	-0.89
JJZ-8-15	142	0.118205	0.003511	0.282428	0.000020	0.282418986	-12.6	-9.79	1247	1791	-0.89

注:测试单位为背景燕都中实测试技术有限公司;测试方法:MC-ICP-MS;实验仪器:Neptune Plus。

表明金井咀矿床闪长岩与矿集区内同时代矽卡岩型金矿具有类似的岩石成因及岩浆源区。但是,金井咀矿床金矿体主要赋存在矿区闪长岩顶部接触带、呈不规则不完整的环筒形围绕在似筒状小岩体内侧或呈脉状分布于小岩体中部。这与其他矿床主要赋存在碳酸盐岩地层或岩体内外接触带明显不同。虽然目前对于金井咀矿床就位特殊性的原因以及区域内是否存在类似矿床尚不明确,但是金井咀矿床的发现,对于完善区域成矿规律,指导金矿找矿勘查具有一定的借鉴意义。

## 6 结 论

(1)金井咀闪长岩具有相对较高的 $^{87}\text{Sr}/^{86}\text{Sr}$ 初始比值,负的 $\varepsilon_{\text{Nd}}(t)$ 值( $-5.24\sim-4.76$ ),显示出富集地幔来源的特征。锆石 $^{176}\text{Hf}/^{177}\text{Hf}$ 值介于0.282360~0.282526, $\varepsilon_{\text{Hf}}(t)$ 值介于-12.2~-6.5,表明岩浆侵位过

程中存在一定程度的地壳混染。

(2)金井咀矽卡岩型金矿床与鄂东南矿集区矽卡岩型金矿床具有相同的成岩成矿时代和类似的岩石成因及岩浆源区。但不同的是,该矿床金矿体主要就位于闪长岩体内部而不是赋存在碳酸盐岩地层或岩体内外接触带。

**致谢:**野外工作得到了中国冶金地质总局中南地质勘查院湖北分院和金井咀矿区工作人员的大力协助,地质背景及矿床地质部分参考了苏欣栋等人研究报告,在此表示感谢。

## Reference

- Amelin Y, Lee D C, Halliday A N, Pidgeon R T. 1999. Nature of the Earth's earliest crust from hafnium isotopes in single detrital zircons[J]. Nature, 399: 252~255.
- Chang Yinfo, Liu Xiangpei, Wu Yanchang. 1991. The Copper Iron Belt of the Lower and Middle Reaches of the Changjiang River[M].

- Beijing: Geological Publishing House, 1–379 (in Chinese).
- Chen Fuwen, Mei Yuping, Li Huaqin. 2011. SHRIMP U–Pb zircon dating for granodiorite porphyry of the Fengshan orefield in eastern Hubei Province and its geological significance[J]. *Acta Geologica Sinica*, 85(1): 88–96 (in Chinese with English abstract).
- Chen Wen, Ruan Qilin, Yang Weiwei, Li Jun, Ke Yufu, Fan Zhonglin, Zhai Si. 2012. Geological characteristics and genesis of Skarn type gold deposit in Jinjingzui, East Hubei Province[J]. *China Mining Magazine*, 21(4): 56–59 (in Chinese with English abstract).
- Ding Lixue, Huang Guicheng, Xia Jinlong. 2018. Age and petrogenesis of the Echeng intrusion in southeastern Hubei Province: Implications for iron mineralization[J]. *Earth Science*, 43(7): 2350–2369 (in Chinese with English abstract).
- Elhlou S, Belousova E, Griffin W L, Pearson W L, O'Reilly S Y. 2006. Trace element and isotopic composition of GJ red zircon standard by laser ablation[J]. *Geochimica et Cosmochimica Acta*, 70(18): A158.
- Falloon T J, Green D H, O'Neill, H S C, Hibberson W O. 1997. Experimental tests of low degree peridotite partial melt compositions: Implications for the nature of anhydrous near-solidus peridotite melts at 1 GPa[J]. *Earth and Planetary Science Letters*, 152 (1/4): 149–162.
- Gong Xuejing, Zeng Jianhui, Cao Dianhua. 2019. Sr–Nd and zircon Hf–O isotopic constraints on the petrogenesis of the orebearing granitic porphyry at Lengshuikeng, Jiangxi Province[J]. *Geology in China*, 46(4): 818–831 (in Chinese with English abstract).
- Hamelin C, Dosso L, Hanan B, Barrat J A. 2010. Sr–Nd–Hf isotopes along the Pacific Antarctic Ridge from 41 to 53°S[J]. *Geophysical Research Letters*, 37(10): 1–5.
- Ji Min, Zhao Xinfu, Zeng Liping, Fan Tianweiteng. 2018. Microtexture and geochemistry of garnets from Tonglushan skarn Cu–Fe deposit in the southeastern Hubei metallogenic province: Implications for ore forming process[J]. *Acta Petrologica Sinica*, 34(9): 2716–2732 (in Chinese with English abstract).
- Li Jianwei, Deng Xiaodong, Zhou Meifu, Liu Yongsheng, Zhao Xinfu, Guo Jingliang. 2010. Laser ablation ICP–MS titanite U–Th–Pb dating of hydrothermal ore deposits: A case study of the Tonglushan Cu–Fe–Au skarn deposit, SE Hubei Province, China[J]. *Chemical Geology*, 270: 56–67.
- Li Jianwei, Zhao Xinfu, Zhou Meifu, Vasconcelos P, Ma Changqian, Deng Xiaodong, Sérgio de Souza, Zhao Yongxin, Wu Gang. 2008. Origin of the Tongshankou porphyry–skarn Cu–Mo deposit, eastern Yangtze craton, Eastern China: Geochronological, geochemical, and Sr–Nd–Hf isotopic constraints[J]. *Mineralium Deposita*, 43: 319–336.
- Li Xinhao, Xie Guiqing, Li Wei, Zheng Xianwei, Liu Mao. 2018. Geological characteristics, U–Pb age and Hf isotope of zircon in hosting intrusion for Baotuanshan Au–Cu deposit, Edong ore cluster and its geological significance[J]. *Geological Bulletin of China*, 37(7): 1346–1359 (in Chinese with English abstract).
- Li Xinhao, Xie Guiqing. 2018. Discussion on metallogenic mechanism of Jinjingzui porphyry gold deposit in Hubei Province [C]// Chinese Geophysical Society (ed.). *Proceedings of the China Geosciences Joint Academic Annual Conference (40)*. Beijing: China Heping Audio–visual and Electronic Publishing House, 1–3 (in Chinese).
- Ling Mingxing, Wang Fangyue, Ding Xing, Hu Yanhua, ZhouJibin, Zartman R E, Yang Xiaoyong, Sun Weidong. 2009. Cretaceous ridge subduction along the Lower Yangtze River belt, Eastern China[J]. *Economic Geology*, 104: 303–321.
- Mao Jingwen, Xie Guiqing, Chao Duan, Pirajno F, Ishiyama D, Chen Yuchuan. 2011. A tectono–genetic model for porphyry–skarn Cu–Au–Mo–Fe and magnetite–apatite deposits along Middle–Lower Yangtze River Valley, Eastern China[J]. *Ore Geology Review*, 43: 294–314.
- Pan Yuanming, Dong Ping. 1999. The Lower Changjiang (Yangzi/Yangtze River) metallogenic belt, East China: Intrusion– and wall rock–hosted Cu–Fe–Au, Mo, Zn, Pb, Ag deposits[J]. *Ore Geology Reviews*, 15: 177–242.
- Pang Ajuan, Li Shengrong, Santosh M, Yang Qingyu, Jia Baojian, Yang Chengdong. 2014. Geochemistry, and zircon U–Pb and molybdenite Re–Os geochronology of Jilongshan Cu–Au deposit, southeastern Hubei Province, China[J]. *Geological Journal*, 49(1): 52–68.
- Samake B, Xu Xiaoming, Jiang Shaoyong. 2018. Oxygen fugacity, temperature and pressure estimation from mineral chemistry of the granodiorite porphyry from the Jilongshan Au–Cu deposit and the Baiguoshu prospecting area in SE Hubei Province: A guide for mineral resource exploration[J]. *Journal of Geochemical Exploration*, 184: 136–149.
- Shu Quanan, Chen Peiliang, Cheng Jianrong. 1992. *Geology of Iron–Copper Deposits in Eastern Hubei Province, China*[M]. Beijing: The Metallurgic Industry Press, 1–510 (in Chinese).
- Su Xindong. 1996. Geological characteristics of the first altered diorite tubular gold deposit in China[J]. *Geology and Exploration*, (3): 1–6 (in Chinese).
- Vervoort J D, Pachelt P J, Gehrels G E, Nutman A P. 1996. Constraints on early Earth differentiation from hafnium and neodymium isotopes[J]. *Nature*, 379(6566): 624–627.
- Wang Qiang, Zhao Zhenhua, Bao Zhiwei, Xu Jifeng, Liu Wei, Li Chaofeng, Bai Zhenghua, Xiong Xiaolin. 2004. Geochemistry and petrogenesis of the Tongshankou and Yinzu adakitic intrusive rocks and the associated porphyry copper–molybdenum mineralization in southeast Hubei, East China[J]. *Resource Geology*, 54: 137–152.
- Xie Guiqing, Mao Jingwen, Li Ruiling, Zhang Zusong, Zhao Weichao,

- Qu Wenjun, Zhao Caisheng, Wei Shikun. 2006. Metallogenic epoch and geodynamic framework of Cu–Au–Mo–(W) deposits in Southeastern Hubei Province: Constraints from Re–Os molybdenite ages[J]. *Mineral Deposits*, 25(1): 43–52 (in Chinese with English abstract).
- Xie Guiqing, Mao Jingwen, Zhao Haijie. 2011a. Zircon U–Pb geochronological and Hf isotopic constraints on petrogenesis of Late Mesozoic intrusions in the southeast Hubei Province, Middle–Lower Yangtze River belt (MLYRB), East China[J]. *Lithos*, 125(1/2): 693–710.
- Xie Guiqing, Mao Jingwen, Zhao Haijie, Wei Ketao, Jin Shangguang, Pan Huijun, Ke Yufu. 2011b. Timing of skarn deposit formation of the Tonglushan ore district, southeastern Hubei Province, Middle–Lower Yangtze River valley metallogenic belt and its implications[J]. *Ore Geology Reviews*, 43(1): 62–77.
- Xie Guiqing, Mao Jingwen, Li Ruiling, Jiang Guohao, Zhao Caisheng, Zhao Haijie, Hou Kejun, Pan Huaijun. 2008.  $^{40}\text{Ar}$ – $^{39}\text{Ar}$  phlogopite dating of large skarn Fe deposits and tectonic framework in southeastern Hubei Province, Middle–Lower Reaches of the Yangtze River, Eastern China[J]. *Acta Petrologica Sinica*, 24(8): 1917–1927 (in Chinese with English abstract).
- Xie Guiqing, Zhao Haijie, Zhao Caisheng, Li Xiangqian, Hou Kejun, Pan Huaijun. 2009. Re–Os dating of molybdenite from Tonglushan ore district in southeastern Hubei Province, Middle–Lower Yangtze River belt and its geological significance[J]. *Mineral Deposits*, 28(3): 227–239 (in Chinese with English abstract).
- Yang Yizheng, Long Qun, Siebel W, Cheng Ting, Hou Zhenhui, Chen Fukun. 2014. Paleo–Pacific subduction in the interior of eastern China: Evidence from adakitic rocks in the Edong–Jiurui district[J]. *The Journal of Geology*, 122: 77–97.
- Yao Lei, Xie Guiqing, Lü Zhicheng, Zhao Caisheng, Wang Jian, Zheng Xianwei, He Zhefeng, Li Wei. 2013. Zircon U–Pb ages, geochemistry and Hf isotopes of granitoids and diorite in the Chengchao Fe deposit in southeastern Hubei ore cluster and its significance[J]. *Journal of Jilin University (Earth Science Edition)*, 43(5): 1393–1422 (in Chinese with English abstract).
- Zhang Shitao, Chen Huayong, Han Jinsheng, Zhang Yu, Chu Gaobin, Wei Ketao, Zhao Yijun, Cheng Jiamin, Tian Jing. 2018. Geochronology, geochemistry, and mineralization of quartz monzodiorite and quartz monzodiorite porphyry in Tonglushan Cu–Fe–Au deposit, Edongnan ore district, China[J]. *Geochimica*, 47(3): 240–256 (in Chinese with English abstract).
- Zhou Taofa, Fan Yu, Wang S W, White N C. 2017. Metallogenic regularity and metallogenic model of the Middle Lower Yangtze River valley metallogenic belt[J]. *Acta Petrologica Sinica*, 33(11): 3353–3372 (in Chinese with English abstract).
- Zhou Taofa, Wang Shiwei, Fan Yu, Yuan Feng, Zhang Dayu, White N C. 2015. A review of the intracontinental porphyry deposits in the Middle Lower Yangtze River valley metallogenic belt, eastern China[J]. *Ore Geology Reviews*, 65: 433–456.
- ### 附中文参考文献
- 常印佛, 刘湘培, 吴言昌. 1991. 长江中下游铁铜矿成矿带[M]. 北京: 地质出版社, 1–379.
- 陈富文, 梅玉萍, 李华芹. 2011. 鄂东丰山矿田花岗闪长斑岩体锆石SHRIMP–Pb定年及其意义[J]. *地质学报*, 85(1): 88–96.
- 陈文, 阮启林, 杨伟卫, 李均, 柯于富, 范中林, 翟思. 2012. 湖北省鄂东地区金井咀矽卡岩型金矿地质特征及其成因[J]. *中国矿业*, 21(4): 56–59.
- 丁丽雪, 黄圭成, 夏金龙. 2018. 鄂东南地区鄂城岩体的时代、成因及其对成矿作用的指示[J]. *地球科学*, 43(7): 2350–2369.
- 龚雪婧, 曾建辉, 曹殿华. 2019. 江西冷水坑矿床含矿花岗斑岩的Sr–Nd及锆石Hf–O同位素研究[J]. *中国地质*, 46(4): 818–831.
- 纪敏, 赵新福, 曾丽平, 范田纬腾. 2018. 鄂东南铜绿山矿床石榴子石显微结构及微区成分对成矿过程的指示[J]. *岩石学报*, 34(9): 2716–2732.
- 李新昊, 谢桂青, 李伟, 郑先伟, 刘茂. 2018. 鄂东矿集区宝团山金铜矿床地质特征、赋矿岩体锆石U–Pb年龄和Hf同位素组成及其地质意义[J]. *地质通报*, 37(7): 1346–1359.
- 李新昊, 谢桂青. 2018. 湖北省金井咀斑岩型金矿成矿机制探讨[C]//中国地球物理学会主编. 中国地球科学联合学术年会论文集(四十). 北京: 中国和平音像电子出版社, 1–3.
- 舒全安, 陈培良, 程建荣. 1992. 鄂东铁铜矿产地质[M]. 北京: 冶金工业出版社, 1–532.
- 苏欣栋. 1996. 我国首例蚀变闪长岩岩筒型金矿地质特征[J]. *地质与勘探*, (3): 1–6.
- 谢桂青, 毛景文, 李瑞玲, 蒋国家, 赵财胜, 赵海杰, 侯可军, 潘怀军. 2008. 鄂东南地区大型矽卡岩型铁矿床金云母 $^{40}\text{Ar}$ – $^{39}\text{Ar}$ 同位素年龄及其构造背景初探[J]. *岩石学报*, 24(8): 1917–1927.
- 谢桂青, 毛景文, 李瑞玲, 张祖送, 赵维超, 屈文俊, 赵财胜, 魏世昆. 2006. 鄂东南地区Cu–Au–Mo–(W)矿床的成矿时代及其成矿地球动力学背景探讨: 辉钼矿Re–Os同位素年龄[J]. *矿床地质*, 25(1): 43–52.
- 谢桂青, 赵海杰, 赵财胜, 李向前, 侯可军, 潘怀军. 2009. 鄂东南铜绿山矿田矽卡岩型铜铁金矿床的辉钼矿Re–Os同位素年龄及其地质意义[J]. *矿床地质*, 28(3): 227–239.
- 姚磊, 谢桂青, 吕志成, 赵财胜, 王建, 郑先伟, 何哲峰, 李伟. 2013. 鄂东南程潮铁矿床花岗质岩和闪长岩的岩体时代、成因及地质意义—锆石年龄、地球化学和Hf同位素新证据[J]. *吉林大学学报(地球科学版)*, 43(5): 1393–1422.
- 张世涛, 陈华勇, 韩金生, 张宇, 初高彬, 魏克涛, 赵逸君, 程佳敏, 田京. 2018. 鄂东南铜绿山大型铜铁金矿床成矿岩体年代学、地球化学特征及成矿意义[J]. *地球化学*, 47(3): 240–256.
- 周涛发, 范裕, 王世伟, Noel C White. 2017. 长江中下游成矿带成矿规律和成矿模式[J]. *岩石学报*, 33(11): 3353–3372.